

## Resonant photoemission shake-up and Auger processes at the $3p$ photothreshold in Ga and GaP

T.-C. Chiang and D. E. Eastman

*IBM Thomas J. Watson Research Center, P.O. Box 218, Yorktown Heights, New York 10598*

(Received 6 December 1979)

Resonant photoemission  $3d^8$  shake-up satellites in Ga metal and GaP, which are closely related to  $M_{2,3}M_{4,5}M_{4,5}$  Auger transitions, have been observed at the  $3p$  photothreshold of Ga. By analyzing the line positions, multiplet structure, and resonant behavior near threshold, we have determined the excitonic binding energies and correlation energies for various one-hole and two-hole excited states. While these two-hole excitations in Ga metal and GaP are similar because of their quasiatomic nature, important differences are observed which are due to different final-state screening mechanisms for a metal and an insulator. The present results are compared with those for Cu and Ni.

### I. INTRODUCTION

Resonant photoemission shake-up, direct recombination, and Auger processes near core-level photothresholds have attracted recent attention.<sup>1-3</sup> Guillo *et al.*<sup>3</sup> observed resonant behavior of the 6 eV satellite of the  $3d$  photoemission peak of Ni near the  $3p$  core-level threshold; they explained the results in terms of configuration interaction and Fano resonance, and inferred a narrow, partially filled  $3d$  band was necessary for such effect. Recently, Iwan, Himpfel, and Eastman<sup>1</sup> have observed a similar phenomenon in Cu, which has a filled  $3d$  shell. Based upon an analysis of the satellite multiplet structure and the resonant behavior at the  $3p$  photothreshold, they have concluded that for both Cu and Ni the satellite is due to a two-electron excitation process in which two  $3d$  electrons are excited simultaneously to generate a photoelectron and a quasi-bound (mainly  $4s$  for Cu and  $3d$  for Ni) electron. For Cu the resonance of the partial cross section of the satellite is attributed to a  $3p$  to unfilled  $4s$  transition. A related study of quasimatrix isolated Cu in Cu-phthalocyanine has been carried out and the results have been explained using an atomic model.<sup>2</sup>

The objective of the present study is to provide a deeper insight of these resonance phenomena by comparing a semiconductor (GaP) with a related metal (Ga). Namely, there are important differences in screening, e.g., dielectric screening versus metallic screening, as well as in the nature of the final states, e.g., band gap (GaP) versus no band gap (Ga). Because the electronic band structures of Ga metal and GaP are well known, important many-body quantities such as the correlation energies, excitation binding energies, etc., can be derived from the experimental results. Atomic Ga has the electronic configuration  $(Ar)3d^{10}4s^24p$  with filled  $4s$  and  $3d$  shells, and

resonant  $3p \rightarrow 3d, 4s$  excitations at the  $3p$  photothreshold are not allowed. However, for GaP, GaSb, and metallic Ga, band-structure effects mix several configurations of nearly the same energy, and resonant two-electron  $3d^8$  excitations similar to those observed in Cu and Ni are observed. In contrast to Cu and Ni, undetectable satellite intensities ( $\leq 1\%$  of the  $3d^9$  main line) are observed away from resonance. Near resonance, new photoemission features appear; a satellite line with multiplet structure corresponding to a  $3d^8$  configuration is clearly observed, including both the strong  $^1G$  and  $^3F$  terms as well as the weak  $^1D$  and  $^1S$  terms which have not been observed for Cu and Ni. The overall resonant behavior is very similar for metallic Ga and semiconducting GaP since it is quasiatomic in nature. However, there are important differences, e.g., a core exciton<sup>4,5</sup> resonance strongly enhances the satellite emission in GaP relative to Ga metal. The two-hole effective Coulomb interactions  $U$  for the  $3d^8$  satellite and Auger structures are the same for Ga metal but differ by  $\sim 1$  eV for GaP.

### II. EXPERIMENT

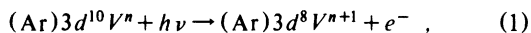
Experiments were done using synchrotron radiation at the Synchrotron Radiation Center at the University of Wisconsin-Madison. A double-stage cylindrical mirror analyzer was used in the angle-averaging mode to analyze the photoelectron energy. The experimental chamber had a working pressure of about  $7 \times 10^{-11}$  Torr.

The solid metallic Ga sample was prepared by cooling down liquid Ga of 99.9999% purity to room temperature in a Ta boat. It was cleaned before measurement by *in situ* scraping using a carbide knife. The cleanliness was monitored using photoemission

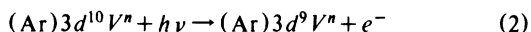
and Auger spectroscopy. The sample could be used for about three hours before detectable amount of indium impurity diffused from the bulk to the surface. The semiconductor samples were *p*-type GaP and GaSb cleaved *in situ* to expose the (110) surfaces; the sample lifetimes were longer than several days.

### III. RESULTS AND DISCUSSIONS

Typical photoelectron energy distribution curves for GaP are shown in Fig. 1. The valence bands and the Ga 3*d* core levels at  $-18.6$  eV (spin-orbit splitting  $\cong 0.5$  eV unresolved) and the associated surface and one and two bulk plasmon loss peaks are well known.<sup>6</sup> As  $h\nu$  is tuned near the 3*p* threshold, sharp features with fixed line shapes and binding energies appear, which correspond to excited Ga (Ar)3*d*<sup>8</sup>*V*<sup>*n*+1</sup> configuration; these are due to a two-electron excitation of Ga atoms with the ground-state configuration (Ar)3*d*<sup>10</sup>*V*<sup>*n*</sup>, where *V* denotes the 4*s* and 4*p* valence charges, that is,



with the electron which is promoted from 3*d* to valence charge mainly in the atomic 4*s* orbital. This is usually called the satellite, or shake-up, line of the 3*d* main emission line which is described by



because (Ar)3*d*<sup>8</sup>*V*<sup>*n*+1</sup> can be considered as a shake-up excitation of the one-electron (Ar)3*d*<sup>9</sup>*V*<sup>*n*</sup> configura-

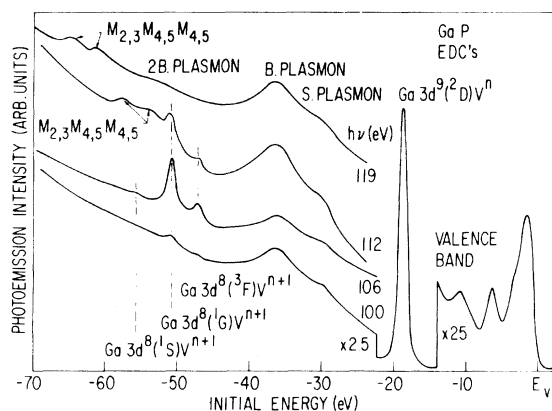
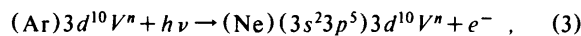


FIG. 1. Typical photoelectron energy distribution curves (EDC's) for GaP (110) surface. Ga 3*d* main emission line and its satellite are denoted by their final-state configurations as 3*d*<sup>9</sup>*V*<sup>*n*</sup> and 3*d*<sup>8</sup>*V*<sup>*n*+1</sup>, respectively, with the term designations (<sup>2</sup>*D*, <sup>3</sup>*F*, <sup>1</sup>*G*, etc.) given. S, B, and 2B plasmons are surface, one bulk, and two bulk plasmon loss peaks, respectively. Peaks labeled *M*<sub>2,3</sub>*M*<sub>4,5</sub>*M*<sub>4,5</sub> are Auger peaks derived from Ga. Initial energy is referred to the valence-band maximum *E*<sub>*V*</sub>.

tion. This satellite assignment is based upon its multiplet structure, resonant behavior near the Ga 3*p* core-level threshold, and similarity to the 3*d*<sup>8</sup> satellite structure observed for Cu.<sup>1,2</sup> Above  $h\nu \cong 110$  eV, the Ga derived *M*<sub>2,3</sub>*M*<sub>4,5</sub>*M*<sub>4,5</sub> Auger lines with constant kinetic energies are clearly observed; these can be described by the photoexcitation and Auger decay processes,



From Eqs. (1) and (4), both the Auger and the two-electron excitation (satellite) lines involve a 3*d*<sup>8</sup> final configuration. Following Refs. 1, 2, and 7, this can be decomposed into *d*<sup>8</sup> multiplet terms: <sup>3</sup>*F*, <sup>1</sup>*D*, <sup>3</sup>*P*, <sup>1</sup>*G*, and <sup>1</sup>*S*. The satellite line shape for GaP are shown<sup>8</sup> in Fig. 2 together with a scale for the correlation energy *U*, which is defined as the difference between the measured energy and that expected from an algebraic sum of one-body energies (to be discussed in detail). For Ga metal,  $h\nu$ -dependent pho-

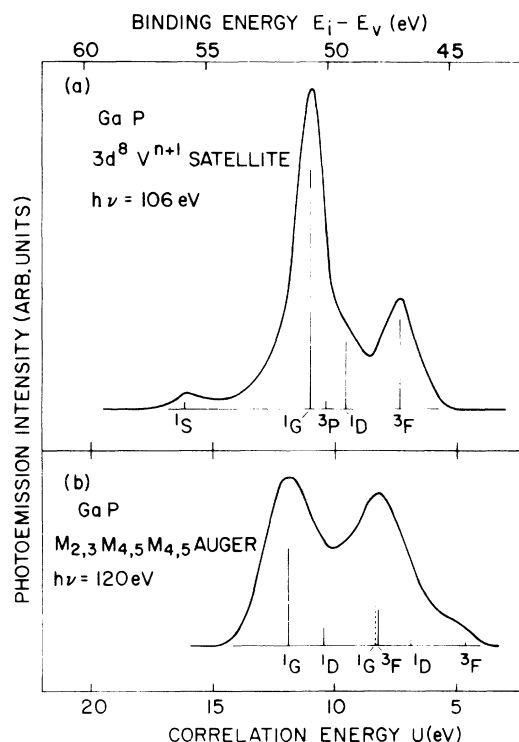
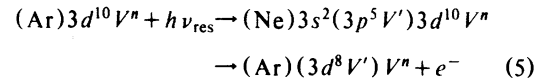


FIG. 2. Line shapes of (a) the satellite structure and (b) the *M*<sub>2,3</sub>*M*<sub>4,5</sub>*M*<sub>4,5</sub> Auger transition for GaP seen in Fig. 1 after background subtraction. They are decomposed into multiplet terms; the heights of the vertical lines represent the relative intensities of the different terms. In (b), the solid and dashed lines are for *M*<sub>3</sub>*M*<sub>4,5</sub>*M*<sub>4,5</sub> and *M*<sub>2</sub>*M*<sub>4,5</sub>*M*<sub>4,5</sub> Auger transitions, respectively, and the weaker <sup>1</sup>*S* and <sup>3</sup>*P* terms are neglected. The correlation energy *U* is defined in the text.

toelectron spectra exhibit Ga-derived satellite and Auger line shapes which are very similar to those observed for GaP (see Figs. 1 and 2).<sup>9</sup> The relevant binding energies for GaP and Ga metal are listed in Table I; they are all defined as positive quantities.

We will discuss the results for GaP first. The partial cross sections of the 3*d* main line (squares) and the satellite line (circles) are shown in Fig. 3 as functions of the photon energy. The partial yield of slow secondary electrons, which is shown as a solid curve, is similar to the absorption coefficient.<sup>10</sup> All the above have been normalized to the  $h\nu$ -dependent incident flux. Two prominent resonance peaks are observed at  $h\nu = 106.5$  and  $110.0$  eV; the separation of 3.5 eV corresponds closely to the spin-orbit splitting of the  $3p_{3/2}$  and  $3p_{1/2}$  core levels of Ga. Within an one-electron picture, the resonance occurs by photoexciting a  $3p$  core electron into a level  $\sim 2.6$  eV above the valence-band maximum (VBM); here we have used the binding energies of the  $3p$  core levels from Table I. The lowest conduction-band critical points in GaP are  $X_{1}^c$ ,  $L_{1}^c$ , and  $\Gamma_{1}^c$  at 2.3, 2.6, and 2.8

eV above VBM, respectively.<sup>11-13</sup> The electric dipole transition moment<sup>14</sup> is very small at  $X_{1}^c$ , medium at  $L_{1}^c$ , and large at  $\Gamma_{1}^c$ , therefore we assign the resonance as due to the formation of a core exciton<sup>4,5</sup> involving a  $3p$  hole and a screening electron near  $\Gamma_{1}^c$  or  $L_{1}^c$ . The small difference in energy of 0.2 eV may be due to a core exciton binding energy and/or band dispersion effects (the  $3p_{3/2}$ ,  $3p_{1/2}$  core levels of Ga are more than 2 eV wide), but since our experimental accuracy is only 0.2 eV, we will ignore this exciton binding energy (estimated to be no greater than 0.2 eV).<sup>14</sup> This resonant  $3p$  photoexcitation at threshold is coupled to various channels via Coulomb interactions. Roughly speaking, direct recombination<sup>15,16</sup> of the  $3p$  excitation results in the enhancement of the 3*d* main emission line while Auger deexcitation results in the enhancement of the satellite line.<sup>1-3</sup> The latter process is described by



where  $V'$  denotes the screening electron near  $\Gamma_{1}^c$  or  $L_{1}^c$ . Rigorously speaking, the final-state wave function with resonant excitation is given by a linear combination in the configuration interaction picture

$$\begin{aligned} \psi_f = &a\psi[(\text{Ne})3s^2(3p^5V')3d^{10}V^n] \\ &+ b\psi[(\text{Ar})3d^9V^n + e^-] \\ &+ c\psi[(\text{Ar})(3d^8V')V^n + e^-] + \dots \end{aligned} \quad (6)$$

TABLE I. Experimentally determined binding energies, satellite resonance energies, and correlation energies for GaP and Ga metals.

	Ga in GaP	Ga metal
Binding energy (eV)		
Reference	Valence-band maximum	Fermi level
$3d_{5/2}$	18.4(1)	18.38(5)
$3d_{3/2}$	18.8(1)	18.83(5)
$(3d)_{\text{av}}$	$(18.6(1))_{\text{av}}$	$(18.53(5))_{\text{av}}$
Satellite:		
$3d^8(^3F)$	47.0(1)	45.2(1)
$^1D$	...	...
$^3P$	...	...
$^1G$	50.7(1)	48.88(5)
$^1S$	55.85(10)	...
$3p$	$3p_{3/2}$	103.9(2)
	$3p_{1/2}$	107.5(2)
Satellite resonance peak energy (eV)		
$3p_{3/2}$	106.5(1)	
$\rightarrow \Gamma_{1}^c(L_{1}^c)$ exciton		
$3p_{1/2}$	110.0(1)	
$3p_{3/2}$		104.2(2)
$\rightarrow$ Fermi level		
$3p_{1/2}$		...
Correlation energy $U$ (eV)		
Satellite $3d^8(^1G)V^{n+1}$	11.0(2)	11.8(1)
Auger $3d^8(^1G)V^n$	11.9(2)	11.8(2)

<sup>a</sup>Reference 20.

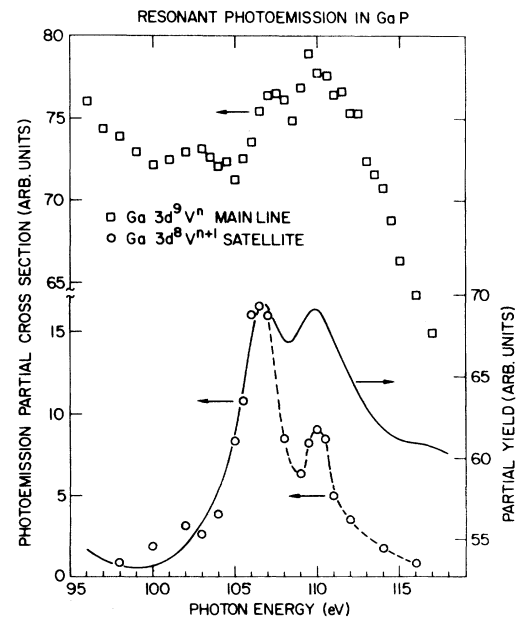


FIG. 3. Partial cross sections of the 3*d* main emission line and its satellite as functions of photon energy for GaP. The dashed curve connects the data points. Also shown is the partial yield as a solid curve.

where the first term describes the  $3p$  photoexcited state (core exciton state), the second term the  $3d$  emission, the third term the satellite emission, and  $a$ ,  $b$ , and  $c$  are appropriate coefficients. Using a perturbation approach, the resonance mainly arises from the electric dipole matrix element connecting the ground state and the core exciton state. As seen in Figs. 1 and 3, the satellite intensity is negligible away from resonance. In this case the coupling between the second term and the third term (nonresonant shake-up) is negligible. With a negligible interference coming from the nonresonant part, the spectral peaks in Fig. 3 for the intensity of the satellite clearly mark the centers of core exciton resonances as listed in Table I. The shapes of the absorption coefficient and the  $3d$  main emission intensity in Fig. 3 do not show strong characteristic Fano profiles, as seen for transition metals,<sup>16</sup> although weak interference effects may be present.

If there were no electron-electron correlation, the satellite state  $\psi[(Ar)(3d^8V')V^n]$  should have a binding energy given by

$$E(3d) + [E(V') + E(3d)] , \quad (7)$$

with all single-particle binding energies (positive)<sup>17</sup> referred to VBM and  $E(V')$  as given below. We take the one-hole state binding energy  $E(3d) = 18.6$  eV to be the average of the two spin-orbit split components, since this splitting is not resolved in our experiment. As discussed previously, we ignore the small core exciton binding energy and thus have

$$E(V') = 2.6 \text{ eV} . \quad (8)$$

The correlation energy  $U_S$  for the satellite is, by definition

$$U_S = E_S - \{E(3d) + [E(V') + E(3d)]\} , \quad (9)$$

where  $E_S$  is the measured binding energy of the satellite referred to VBM.  $U_S$  for the strongest  $^1G$  term is 11.0 eV, as listed in Table I. The final state for the  $M_{2,3}M_{4,5}M_{4,5}$  Auger transition is a pair of  $3d$  holes in the solid with the surrounding medium polarized, and two electrons (one photoelectron and one Auger electron) excited into the continuum as given by Eqs. (3) and (4). The binding energy of the final two- $3d$  hole state  $\psi[(Ar)3d^8V^n]$  referred to VBM is given by

$$E_A = h\nu - (E_A^* + \phi) - (E_p^* + \phi) , \quad (10)$$

where  $E_{A,p}^*$  are the kinetic energies of the Auger electron and photoelectron, respectively, and  $\phi$  the photothreshold (vacuum level minus VBM). If hole-hole correlation were neglected, the two-hole state  $\psi[(Ar)3d^8V^n]$  would have a binding energy referred to VBM given by

$$E'_A = 2E(3d) . \quad (11)$$

The correlation energy  $U_A$ , i.e., effective Coulomb

energy<sup>18</sup> for the two-hole state, is given by the difference of  $E_A$  and  $E'_A$

$$\begin{aligned} U_A &= E_A - 2E(3d) \\ &= -(E_A^* + \phi) + [E(3p) - 2E(3d)] , \end{aligned} \quad (12)$$

where we have used Eq. (10) and the relation

$$E_p^* + \phi = h\nu - E(3p) . \quad (13)$$

$E_A^* + \phi$  is easily measured from the spectra and we obtain  $U_A = 11.9$  eV for the strongest  $^1G$  term.  $U_A$  is independent of  $\phi$  as it should be, since this is a bulk phenomenon.

$U_A = 11.9$  eV means it takes 11.9 eV more energy to create a two- $3d$  hole state than to create two separate one- $3d$  hole states. This energy comes from the effective Coulomb repulsion between the two holes. This interaction is called effective, because the one-hole and two-hole states are dressed, i.e., they are states with vacancies in the  $3d$  shell and associated screening configurations. For the satellite, the screening electron resonantly excited to near  $\Gamma_f^c$  or  $L_f^c$  effectively screens the two- $3d$  holes, thus reducing  $U_A$  from 11.9 eV to  $U_S = 11.0$  eV. Consequently, we attribute the change of 0.9 eV in  $U$  to this additional Coulomb attraction between the screening electron and the two deep  $3d$  holes. We envision the satellite state  $\psi[(Ar)(3d^8V')V^n]$  as an excitonic state in a somewhat generalized sense; photoemission from this state leads to the satellite structure with fixed binding energy. Therefore, a partially unfilled narrow  $3d$  band is not necessary to obtain such a satellite.<sup>19</sup>

The above argument with modifications can be extended to account for the results in Ga metal. The  $3d$  main emission (squares) and satellite (circles) intensities for Ga metal are shown in Fig. 4. Also shown is the partial yield of slow secondary electrons, whose spectral features presumably closely resemble those of the absorption spectrum (not available). The satellite intensity is much weaker in Ga metal than in GaP and GaSb. The first resonance peak position for the satellite in Fig. 4 corresponds very well to the  $3p_{3/2}$  binding energy of 104.2 eV referred to the Fermi level<sup>20</sup>; the second peak position cannot be determined accurately because the weak satellite overlaps the Auger lines and the data scattering is large. Nevertheless, the screening electron is resonantly excited from  $3p$  to just above the Fermi level with negligible (excitonic) energy shift involved.<sup>21</sup> The  $3d$  main emission intensity shows a positive slope with no fine structure ( $\leq 0.5\%$ ) near threshold, in sharp contrast to that observed in GaP. The very weak resonant structure observed in the partial yield spectrum have more complicated line shapes, probably due to interference effects.<sup>16,21</sup> Generally, the resonance effect is much weaker in Ga

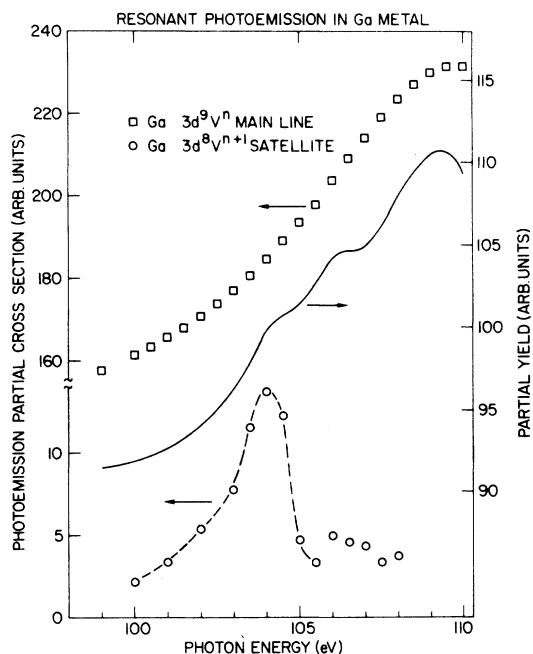


FIG. 4. Same as Fig. 3 except the results are for Ga metal.

metal than in GaP (note the relative vertical scales in Fig. 4).

Individual satellite multiplet lines are somewhat broader in Ga metal than in GaP presumably due to lifetime effects, but the overall multiplet structure is the same as that of GaP. The Auger lines in Ga metal and GaP have similar shapes. Following the procedure described for GaP, the satellite and Auger lines in Ga metal have been decomposed into multiplet terms. With the screening electron at the Fermi level for the satellite, the correlation energies can be calculated in much the same way. Equations (9) and (12) are replaced by

$$U_S = E_S - 2E(3d) \quad (14)$$

and

$$U_A = E_A - 2E(3d) \\ = -(E_A^* + \phi') + [E(3p) - 2E(3d)] \quad (15)$$

where all binding energies are referred to the Fermi level,  $E_A^*$  is the Auger electron kinetic energy and  $\phi'$  (4.2 eV) is the work function. Results for the strongest  $^1G$  term as listed in Table I, where it is seen that  $U_A = U_S = 11.8$  eV.

Metallic screening with a soft Fermi sea is quite different from the polarization screening in a semiconductor; namely, all one-hole and two-hole states are screened in such a metal within approximately a Thomas-Fermi length to form neutral entities.<sup>22</sup> It is clear that the excited  $3d^8$  states of Ga for both Auger and satellite transitions are screened in the same way,

although one unit of screening charge is resonantly excited from the  $3p$  shell for the satellite state. With  $n \rightarrow \infty$  formally in Eqs. (1) and (3)–(5) as appropriate for a macroscopic metallic sample (i.e., a given atomic core feels the whole Fermi sea) and  $V = V'$ , one can see that the final states of the metal are the same for the satellite and Auger transitions, i.e.,  $E_S = E_A$ . With Eqs. (14) and (15), this explains why  $U_A = U_S$  for Ga metal.

We now compare the results for Ga metal and GaP.  $U_A$  is conventionally calculated using approximate wave functions appropriate for a neutral atom, thus  $U_A$  is decomposed into two terms<sup>7,23</sup>

$$U_A = F - R \quad (16)$$

$F$  is the Coulomb energy of the two final  $3d$  holes with relaxation ignored and should be independent of chemical bonding to a good approximation.  $R$ , usually called the static relaxation or total relaxation, is the additional relaxation energy due to the two-hole final state above and beyond the sum of the two one-hole relaxation energies.  $R$  can be further divided into several parts<sup>7,23</sup>: inner-shell, intra-shell, outer-shell, and extra-atomic contributions. In general, the outer-shell and extra-atomic contributions to  $R$  should be sensitive to bonding and the environment. However, as seen in Table I,  $U_A$  is the same for both Ga metal and GaP within experimental error and we thus conclude that  $R$  is also the same in this case.

Finally we consider the maximum satellite intensity relative to the  $3d$  main emission intensity at resonance; results from the present and past experiments<sup>1,2</sup> are shown in Table II. The relative satellite intensity goes down from Ni to Cu as expected due to filling up of the available empty  $3d$  and  $4s$  states. It is also noted that the relative satellite intensities for Ga and Cu are generally greater in a compound than in the pure metal; this point has also been verified in other systems currently under study. From a simple atomic picture point of view, this behavior can be understood as due to charge transfer of the  $4s$  and  $3d$  electrons away from the metal when forming a compound, thus more empty  $4s$  and  $3d$  states are available for resonant excitation.

TABLE II. Maximum satellite intensity relative to the  $3d$  main intensity at resonance.

Metal	Ga <sup>a</sup> 7%	Cu <sup>b</sup> ~15%	Ni <sup>b</sup> ~100%
Compound	GaP <sup>a</sup> 20%	Cu-phthalocyanine <sup>b</sup> 40%	

<sup>a</sup>Present work.

<sup>b</sup>Reference 2.

## ACKNOWLEDGMENTS

The authors are grateful to F. J. Himpsel, M. Iwan, and E. E. Koch for helpful discussions, and to J. J. Donelon, A. Marx, and the staff of the Synchrotron Radiation Center at Stoughton for assistance. This work is supported in part by the U.S. Air Force Office of Scientific Research, Contract No. F44620-76-C-0041.

- 
- <sup>1</sup>M. Iwan, F. J. Himpsel, and D. E. Eastman, *Phys. Rev. Lett.* **43**, 1829 (1979), and references therein.
- <sup>2</sup>M. Iwan, E. E. Koch, T. C. Chiang, D. E. Eastman, and F. J. Himpsel (unpublished).
- <sup>3</sup>C. Guillot, Y. Ballu, J. Paigne, J. Lecante, K. P. Jain, P. Thiry, R. Pinchaux, Y. Petroff, and L. M. Falicov, *Phys. Rev. Lett.* **39**, 1632 (1977).
- <sup>4</sup>M. Altarelli and D. L. Dexter, *Phys. Rev. Lett.* **29**, 1100 (1972).
- <sup>5</sup>A. B. Kunz, *Phys. Rev. B* **12**, 5890 (1975).
- <sup>6</sup>L. Ley, R. A. Pollak, F. R. McFeely, S. P. Kowalczyk, and D. A. Shirley, *Phys. Rev. B* **9**, 600 (1974).
- <sup>7</sup>E. Antonides, E. C. Janse, and G. A. Sawatzky, *Phys. Rev. B* **15**, 1669 (1977).
- <sup>8</sup>With our measured satellite binding energies for <sup>3</sup>F, <sup>1</sup>G, and <sup>1</sup>S, we obtain  $F^2 = 14.39$  and  $F^4 = 7.81$ , where  $F^2$  and  $F^4$  are Coulomb integrals as defined in Ref. 7. Our values are in good agreement with those reported in Ref. 7.
- <sup>9</sup>The Ga-derived satellite and Auger emission features for Ga metal are somewhat weaker ( $\times \frac{1}{3}$ ) and slightly broader than for GaP and, of course, the valence-band emission features are different.
- <sup>10</sup>M. Cardona, W. Gudat, B. Sonntag, and P. Y. Yu, in *Proceedings of the Tenth International Conference on the Physics of Semiconductors, Cambridge, Massachusetts, 1970*, edited by S. P. Keller, J. C. Hensel, and F. Stern (U.S. AEC Division of Technical Information, Springfield, Va., 1970), p. 209. The small discrepancy in peak positions is probably due to different monochromator calibration.
- <sup>11</sup>J. R. Chelikowsky and M. L. Cohen, *Phys. Rev. B* **14**, 556 (1976).
- <sup>12</sup>P. J. Dean, G. Kaminsky, and R. B. Zetterstrom, *Phys. Rev.* **38**, 3551 (1967); D. S. Kyser and V. Rehn, *Phys. Rev. Lett.* **40**, 1048 (1978).
- <sup>13</sup>A. Onton and L. M. Foster, *J. Appl. Phys.* **43**, 5084 (1972).
- <sup>14</sup>D. E. Aspnes, C. G. Olson, and D. W. Lynch, *Phys. Rev. B* **12**, 2527 (1975).
- <sup>15</sup>M. Aono, T.-C. Chiang, J. A. Knapp, T. Tanaka, and D. E. Eastman (unpublished).
- <sup>16</sup>See, for example, G. P. Williams, G. J. Lapeyre, J. Anderson, R. E. Dietz, and Y. Yafet, *J. Vac. Sci. Technol.* **16**(2), 528 (1979).
- <sup>17</sup>The one-hole state energies are measured using photoemission; the effect of relaxation is automatically included.
- <sup>18</sup>This is the same as the effective Coulomb interaction energy defined in Ref. 8.
- <sup>19</sup>See, for example, D. R. Penn, *Phys. Rev. Lett.* **42**, 921 (1979).
- <sup>20</sup>*Topics in Applied Physics*, edited by L. Ley and M. Cardona (Springer-Verlag, Berlin, 1979), Vol. 27, p. 377.
- <sup>21</sup>C. A. Swarts, J. D. Dow, and C. P. Flynn, *Phys. Rev. Lett.* **43**, 158 (1979).
- <sup>22</sup>See, for example, N. D. Lang and A. R. Williams, *Phys. Rev. B* **20**, 1369 (1979).
- <sup>23</sup>S. P. Kowalczyk, R. A. Pollak, F. R. McFeely, L. Ley, and D. A. Shirley, *Phys. Rev.* **8**, 2387 (1973).